Turbulent Flow within a Random Array of Rigid, Emergent Stems: Laboratory Characterization of the Drag Coefficient

Ana M. Ricardo
Instituto Superior Técnico, TULisbon, Portugal & Laboratory of Hydraulic Constructions, EPFLausanne, Switzerland. Email: ana.ricardo@ist.utl.pt

Tiago Silva
Department of Civil Engineering. Faculty of Engineering, U.Porto, Portugal

João Pedro Pêgo
Department of Civil Engineering. Faculty of Engineering, U.Porto, Portugal

Rodrigo Maia
Department of Civil Engineering. Faculty of Engineering, U.Porto, Portugal

Mário J. Franca
Faculty of Sciences and Technology & IMAR- CMA, New University of Lisbon, Caparica, Portugal

Anton Schleiss
Laboratory of Hydraulic Constructions, EPFLausanne, Switzerland

Rui M.L. Ferreira
Instituto Superior Técnico, TULisbon, Portugal

ABSTRACT: Within the bioengineering framework, designing a non-erodible channel is a complex fluid dynamics problem as it involves knowing the drag exerted on the boundary, the drag exerted on the plant stems and the overall friction slope. Most of the existing design criteria employ resistance formulas such as Manning's, calibrated ad hoc. Moving toward physically based design criteria, progresses have been made in the characterization of 3D flows over irregular boundaries, mainly due to the application of Double-Averaging methods (D-AM), which are a particular form of upscaling. Such methods are especially pertinent for the characterization of the flow within and in the near vicinity of plant canopies.This work is aimed at the determination of the drag coefficient associated to rigid emergent stems in turbulent flows. Specific objectives are i) the detailed characterization and quantification of the flow within vegetated areas susceptible to be simulated by dense arrays of vertical emergent stems and ii) the independent quantification of the forces, per unit bed area, acting on the stems and on the bed boundary. Both objectives concur for a better knowledge of the flow resistance in wetlands and vegetated areas in general. To meet the proposed objectives, conditions similar to those found in nature were reproduced in laboratory facilities, using Particle Image Velocimetry (PIV).Since actual wetlands exhibit patchiness and spatial variability in stem density, the experiments featured a periodic distribution of stem densities with minimum and maximum values of 400 and 1600 stems/m^2, respectively. The treatment of the data was done with the Double-Averaging methodology (D-AM), to account for the great spatial variability of the flow. The results reveal that the contribution of form-induced stresses, namely longitudinal and shear stresses is of the order of magnitude of the contribution of Reynolds stresses. Hence, in general, this stresses cannot be neglected. The analysis of form-induced stresses helps to explain the increase of the drag coefficient when the stem density increases.

KEYWORDS: Vegetation, PIV, Double-Averaging Methods, Drag coefficient

1 INTRODUCTION

River engineering works procure not only flood protection but also good practices concerning water quality, habitat diversity and landscape design. Emergent vegetation covering and wetlands has an important role in fluvial ecosystems being able to control the fluxes of sediment, nutrients and

contaminants (Tanino&Nepf 2008). The characteristics of the flow, namely velocities, stresses and fluxes, are strongly dependent on the density and type of vegetation, and exhibit important spatial heterogeneity. The complexity of this kind of flows justifies the smaller body of knowledge,compared to boundary-layer flows. Most of the existing design criteria employ resistance formulas such as Manning's, calibrated *ad hoc*. Moving toward physically based design criteria,progresses have been made in the characterization of 3D flows over irregular boundaries and over canopies, mainly due to the application of double-averaging methods (D-AM), which are a particular form of upscaling in the spatial and temporal sense (Raupach et al. 1986, Gimenez-Curto and CornieroLera 1996, Finnigan 2000 and Nikora et al. 2001, 2007).

Since natural systems are not homogeneous, the flow within the stem array is influenced by several space scales, determined by the number-density of stems and its spatial modulation. The present work features the study of a flow with spatial variability of areal number-density of stems along the streamwise direction. The main objective of study is the determination of the drag coefficient for such demanding conditions. Particular goals include a detailed characterization and quantification of the flow within vegetated areas susceptible to be simulated by dense arrays of vertical emergent stems and the independent quantification of the forces, per unit bed area, acting on the stems and on the bed boundary. These objectives concur for a better knowledge of the flow resistance in wetlands and vegetated areas in general. To meet these objectives, experimental tests were carried out featuring a periodic distribution of stem densities with minimum and maximum values of 400 and 1600 stems/m^2, respectively.

In the next section the equations needed to estimate the drag coefficient under the D-AM framework are presented. This is followed by a description of the experimental setup and instrumentation. Then a qualitative description of the flow is performed, followed by the presentation of the main results. The paper is ended by a set of conclusions.

2 GOVERNING EQUATIONS

To understand flow resistance phenomena in vegetated streams is necessary to resort to a formulation of the momentum and mass conservation equations that take explicitly into account flow variability at inter-stems scale. The Double-Average methodology (D-AM) provides the conceptual framework for the theoretical model for the calculation of the force acting on the stems and, independently, the force acting on the bed surface, derived from the set of flow conservation equations.

The quantification of the additional drag provided by the stems in the studied kind of flows is of great relevance for river engineers, which is often done by means of the drag coefficient. Within the DAM framework, the double-averaged drag coefficient is defined as $C_D = 2\langle \overline{f}_D \rangle / \rho \langle \overline{u} \rangle^2 d$, where $\langle \overline{f}_D \rangle$ is the drag force per unit of submerged stem length, ρ is water density, $\langle \overline{u} \rangle$ is the time and space averaged longitudinal velocity and d is the stem diameter.

The conservation equations of turbulent flows are expressed for time-averaged quantities which, in case of unsteady flow, are defined in a time-window smaller than the fundamental unsteady flow time-scale, and for space averaged quantities, defined in space windows larger than the characteristic wavelength of the boundary irregularities.

The equations of momentum conservation, called within D-AM framework double averaged Navier-Stokes equations (DANS) are defined by (Nikora et al 2001, Ferreira et al 2009)

$$\langle \overline{u}_i \rangle \frac{\partial \langle \overline{u}_j \rangle}{\partial x_i} = -g_j - \frac{1}{\psi\rho}\frac{\partial \psi \langle \overline{p} \rangle}{\partial x_j} - \frac{1}{\psi}\frac{\partial \psi \langle \overline{u_i' u_j'} \rangle}{\partial x_i} - \frac{1}{\psi}\frac{\partial \psi \langle \tilde{u}_i \tilde{u}_j \rangle}{\partial x_i} + \frac{1}{\psi}\frac{\partial}{\partial x_i}\left(\psi \left\langle \nu \frac{\partial \overline{u}_j}{\partial x_i} \right\rangle \right) + \frac{1}{\rho \forall_f^{(s)}} \int_{S_{int}^{(s)}} \overline{p} n_j \partial S - \frac{1}{\forall_f^{(s)}} \int_{S_{int}^{(s)}} \nu \frac{\partial \overline{u}_j}{\partial x_i} n_i \partial S + \frac{1}{\rho \forall_f^{(b)}} \int_{S_{int}^{(b)}} \overline{p} n_j \partial S - \frac{1}{\forall_f^{(b)}} \int_{S_{int}^{(b)}} \nu \frac{\partial \overline{u}_j}{\partial x_i} n_i \partial S \quad (1)$$

where i,j = 1,2,3 are directions of the Cartesian referential, u_j is the j^{th}velocity component,p is pressure, ν is the kinematic viscosity,g_j is the j^{th} gravitational acceleration component and ψ is the void function. Overlines stand for time-average operator while angular brackets stand for space-average operator; primes are time fluctuations and tildes spatial fluctuations. $\forall_f^{(k)}$ and $S_{\text{int}}^{(k)}$ stand, respectively, for the volume

of fluid and the area of the fluid-solid interface of the control volume k (k=s identifies the control volume bounded by bed and the free surface while k=b identifies the control volume bounded by the horizontal plan that contains the crests of the rough bed and the actual bed elevation). $\rho\psi\left\langle\overline{u_i'u_j'}\right\rangle$ represents the space average of well-known Reynolds stress tensor while $\rho\psi\left\langle\tilde{u}_i\tilde{u}_j\right\rangle$ is the form induced stress tensor, which expresses the effect of the spatial variation of the velocity field. The integral terms on equation (1) represent the form and the viscous drag on the stems and on the bed.

The integration of the previous equation in longitudinal direction leads to an equation which allows the computation of the drag force exerted on the stems per unit plan area, $\left\langle\overline{f_x^{(s)}}\right\rangle=\left\langle f_D\right\rangle m\left\langle\overline{h}\right\rangle$ (m stands for stem density and $\left\langle\overline{h}\right\rangle$ is the double-averaged flow depth), when others terms can be accessed by experimental data. To compute stem drag force on the present work several hypothesis and assumptions are needed. Horizontal velocity maps proved that lateral velocity is very small, so it is considered that $\left\langle\overline{v}\right\rangle\approx 0$, also $\left\langle\overline{w}\right\rangle$ is nearly zero throughout the water column. Once stems are vertical and emergent, and assuming that the bed oscillations have a negligible impact on the void function, ψ is considered constant in the control volume and the pressure drag in the vertical direction is zero. Viscous drag at the stems and form induced stresses at the bottom were not assessed. However, they should be of the order of magnitude, or smaller, of the viscous drag at the bottom, which proved to be much smaller than the other terms of the equation. Considering a hydrostatic pressure distribution and incorporating the previous assumptions, equation (1) in the longitudinal direction follows

$$\frac{\partial\left\langle\overline{u}\right\rangle^2}{\partial x}=-g\frac{\partial\left\langle\overline{h}\right\rangle}{\partial x}-\frac{\partial\left(\left\langle\overline{u'^2}\right\rangle+\left\langle\tilde{u}^2\right\rangle\right)}{\partial x}-\frac{\partial\left(\left\langle\overline{u'w'}\right\rangle+\left\langle\tilde{u}\tilde{w}\right\rangle\right)}{\partial z}+\frac{1}{\rho\forall_f^{(s)}}\int_{S_{int}^{(s)}}\overline{p}n_x\,\mathrm{d}S-\frac{1}{\forall_f^{b}}\int_{S_{int}^{b}}\nu\frac{\partial\overline{u}}{\partial z}n_z\,\mathrm{d}S \qquad (2)$$

Integrating in the longitudinal direction the previous equation, introducing the free-surface kinematic boundary condition and normalizing by the leading term $g\left\langle\overline{h}\right\rangle$, it leads to the following expression

$$\frac{\left\langle\overline{f_x^{(s)}}\right\rangle}{\rho g\left\langle\overline{h}\right\rangle}=-\frac{\partial\left\langle\overline{h}\right\rangle}{\partial x}\left(\underbrace{\frac{1}{g\partial\left\langle\overline{h}\right\rangle/\partial x}\frac{\partial U_p^2}{\partial x}}_{\mathrm{A}}+\underbrace{\frac{U_p^2}{g\left\langle\overline{h}\right\rangle}}_{\mathrm{B}}+1+\underbrace{\frac{1}{g\partial\left\langle\overline{h}\right\rangle/\partial x}\frac{\partial\left[\left\langle\overline{u'^2}\right\rangle\right]}{\partial x}}_{\mathrm{D}}+\underbrace{\frac{1}{g\partial\left\langle\overline{h}\right\rangle/\partial x}\frac{\partial\left[\left\langle\tilde{u}^2\right\rangle\right]}{\partial x}}_{\mathrm{E}}\right)$$
$$+\frac{\partial\left\langle\overline{h}\right\rangle}{\partial x}\left(\underbrace{\frac{\left\langle\overline{u'^2}\right\rangle\Big|_{\langle\overline{h}\rangle}-\left[\left\langle\overline{u'^2}\right\rangle\right]+\left\langle\tilde{u}^2\right\rangle\Big|_{\langle\overline{h}\rangle}-\left[\left\langle\tilde{u}^2\right\rangle\right]}{g\left\langle\overline{h}\right\rangle}}_{\mathrm{F}}\right) \qquad (3)$$

where brackets stand for the depth-average operator.With experimental data, the terms of equation (3) are computed in order to quantify the drag coefficient that is presented at results section.

3LABORATORY FACILITIES AND INSTRUMENTATION

The experimental work was carried out in a 12.5 m long and 40.8 cm wide recirculating tilting flume of the Laboratory of Hydraulics and Environment of Instituto Superior Técnico. The flume has glass side walls, enabling flow visualization and laser illumination. A general representation of the flume is shown in Figure 1.

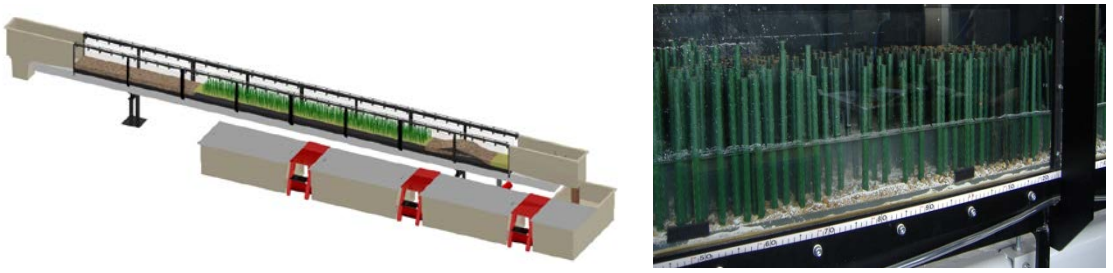

Figure 1 Left: Representation of the tilting recirculation flume at Laboratory of Hydraulics of IST; right: Flume view during experiments.

The flume bottom was covered with a thin horizontal layer of gravel and sand and arrays of rigid, vertical and cylindrical stems were randomly placed along of a 3.5 m long reach simulating emergent vegetation conditions. The diameter of the cylindrical elements is 1.1 cm. The stems were placed in order to create patches with a higher density (≈1600 stems/m^2) alternated with patches of lower density (≈400 stems/m^2). Both of these reaches have the flume width and a length of 15 cm and they are separated by a 10 cm long transition reach where the stem's density is 1200 stems/m^2 along half of the reach and it is 800 stems/m^2 on the another half. Stem density varied periodically with a wavelength of 0.5 m.Figure 2 is a plan view of the downstream part of the vegetation covered reach, which included the 8 longitudinal positions where vertical and horizontal instantaneous maps of velocity were measured. Downstream the reach covered with vegetation, a coarse gravel weir controlled the flow.

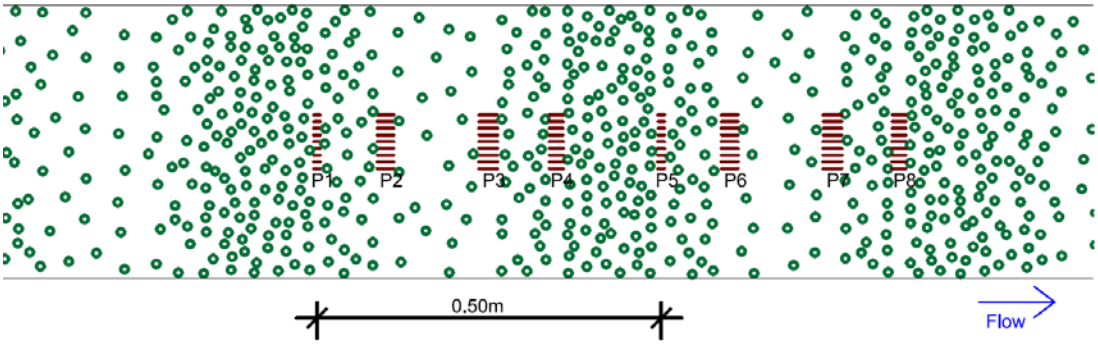

Figure 2 Plan view of part of the vegetation covered reach. The horizontal brown lines represent the positions where the vertical measurements were made on.

The measurements consisted in instantaneous velocity maps acquired with a 2D Particle Image Velocimetry system (PIV) of 30mJ. The PIV is an optical technology that infers fluid's velocity by measuring seeding particle's velocity. The system is composed of laser head, power supply, CCD camera and acquisition system and control and it is based on a double-cavity laser which allows the user to set the delay between two laser pulses. During these experimental tests the PIV was operated at a sampling rate of 15 Hz and with a time between pulses of 1500 μs. Polyurethane seeding particles were employed for flow visualization and measuring. Its specific gravity is 1.31 and the diameters range is from 50 to 70 μm, with 60 μm of mean. Using this seeding, the cut-off frequency of the turbulent signal, calculated with the theory of Hjemfelt and Mockros (1996), is about 40 Hz. Given that the Nyquist frequency of the PIV measurements is 7.5 Hz, it is concluded that the seeding particles are adequate for the performed laboratory work.

For each longitudinal position, represented in Figure 2 (P1-P8), horizontal and vertical, PIV velocity maps were acquired. The PIV vertical measurements were made in 9 vertical planes (identified by horizontal lines on Figure 2). Each PIV data set corresponds to 10×573 image couple, representing a total acquisition time of 6min 22s. Concerning horizontal maps, herein applied only for a qualitative flow characterization, maps of ≈ 9.5 cm long and 12.5 cm wide were acquired at each longitudinal

position,covering the entire flume width. For each acquisition 5000 image couples were collected, corresponding to 5.5 minutes of consecutive data.

3 QUALITATIVE DESCRIPTION OF THE FLOW

Herein a brief description of the flow variables is presented. Table 1 summarizes the main variable for each longitudinal position, where x is the longitudinal coordinate of the measurement section, m is the stem density, U_p stands for the depth averaged of the double-averaged longitudinal velocity where the flow is controlled by the stems, $\mathrm{d}\langle\overline{h}\rangle/\mathrm{d}x$ is the gradient of the mean flow depth and $\mathrm{Re}_p = U_p d/\nu$ is the stem Reynolds number, being d the stem diameter. The experiments were run with a discharge of 2.3 l/s.

Table 1 Features of the experimental tests and flow properties for each longitudinal position.

	P1	P2	P3	P4	P5	P6	P7	P8
x (m)	6.680	6.782	6.935	7.036	7.192	7.293	7.446	7.545
m (stems/m^2)	1600	800	400	1200	1600	800	400	1200
U_p (m/s)	0.082	0.086	0.094	0.100	0.103	0.111	0.107	0.118
$\langle\overline{h}\rangle$ (m)	0.066	0.063	0.062	0.061	0.056	0.054	0.053	0.052
$\mathrm{d}\langle\overline{h}\rangle/\mathrm{d}x$ (-)	-0.014	-0.029	-0.008	-0.010	-0.035	-0.015	-0.009	-0.007
Re_p (-)	902	946	1034	1100	1133	1221	1177	1298

The flow is gradually varied which accelerates in downstream direction as its depth decreases. The free surface exhibited an oscillating behavior, being the amplitude of those oscillations bigger within the patches with higher stem densities. Maps of 2D horizontal mean velocity and maps of mean vorticity (Figure 3) were computed to characterize the flow in the inter-stem region for all the longitudinal positions. The graphs of Figure 3show that the flow within vegetation covered areas evidences a great heterogeneity, at large scales, with lower velocity in the wake of the stems and higher velocity in regions between two stems.These low/high velocity patterns are observed for all thetested stem densities. The time averaged vorticity maps show a repeating symmetricallypaired vortexes pattern caused by the unsteady separation of the flow over the cylinders.These quasi-symmetric high vorticity patterns behind the stems identify Von Kármán vortexstreets. Comparing vorticity maps for the different longitudinal positions, one can concludethat stems induce quite regular structure of vortex patterns independently of the stem density.However, the space necessary to fully develop the vortex pattern is strongly reducedin the higher density. At the lowest stem density patches vorticity has space to decrease itsintensity what is not observed at the highest density regions where the vortices are forcedto compress. From the phenomenological point of view, turbulent structures generation inthis kind of flow is similar to generation in the case of an isolated cylinder, it is a wakeproduction dominated flow. The vortex generation is due to the flow separation around thecylinder, being the size of the vortices dependent on the cylinder diameter. Consequently,the inter-stem space plays a very important role on the turbulent field, since it controlsthe density and the spatial organization of those vortices. Therefore, a patch with a higherstem density, having smaller inter-stem space, leads to higher vortex density which resultsin stronger spatial velocity fluctuations.

Figure 4presents vertical maps of time averaged velocity, exemplifying the data used to compute the double averaged variables presented in the next section. These graphs show that the time-averaged longitudinal velocities are almost constant throughout the water column, except within a thin layer near the bed.

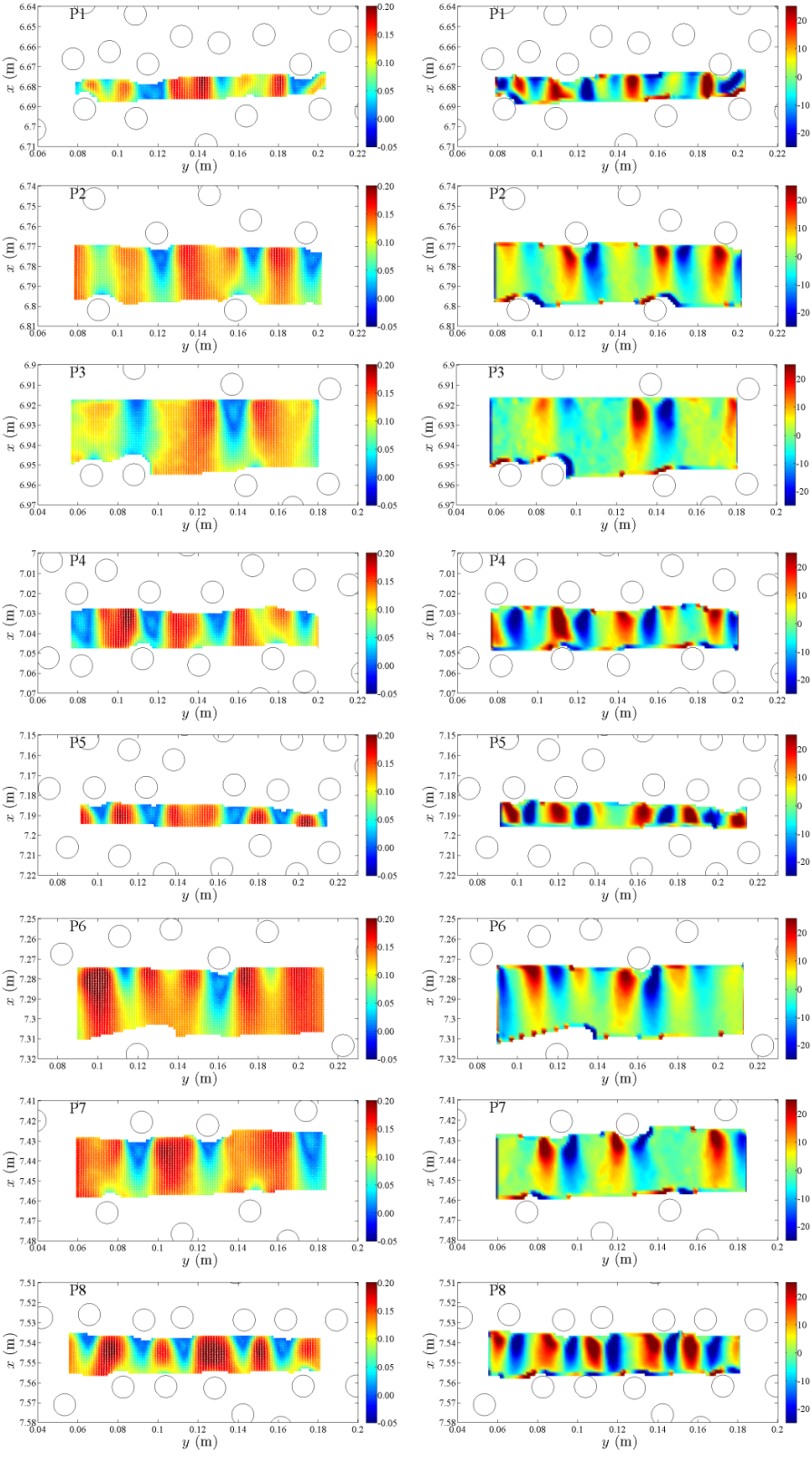

Figure 3 Horizontal maps of time averaged velocity (m/s – left) and vorticity (s^{-1} – right) for allpositions .

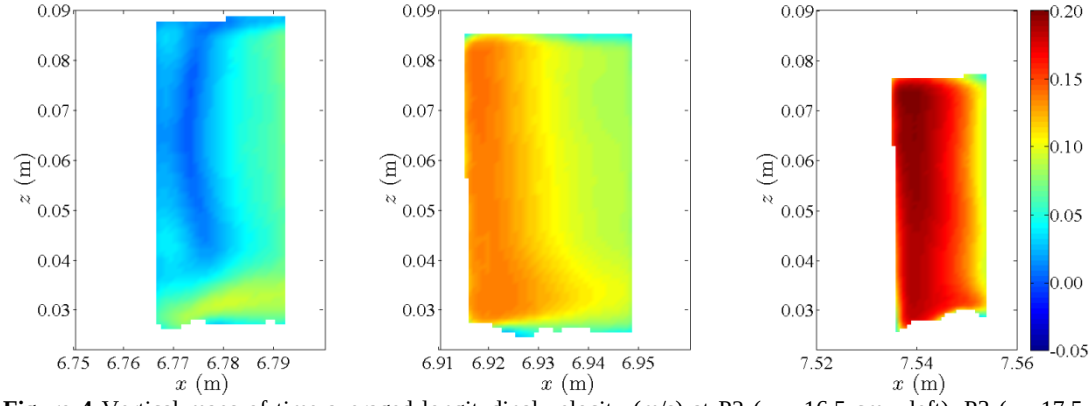

Figure 4 Vertical maps of time-averaged longitudinal velocity (m/s) at P2 (y = 16.5 cm - left), P3 (y= 17.5 cm - middle) and P8 (y = 17.5 cm – right).

4 RESULTS

Data from vertical measurements was time- and space-averaged in order to compare velocities and stresses for each longitudinal position identified in Figure 2, so that the impact of the stem density in the fluid variables could be evaluated.

Figure 5shows profiles of double-averaged longitudinal velocities for each position. One can conclude that this variable is nearly constant in the region where the flow should be mainly controlled by the stems. Furthermore, longitudinal velocity profiles are similar for all the stem densities, from the profile shape point of view.

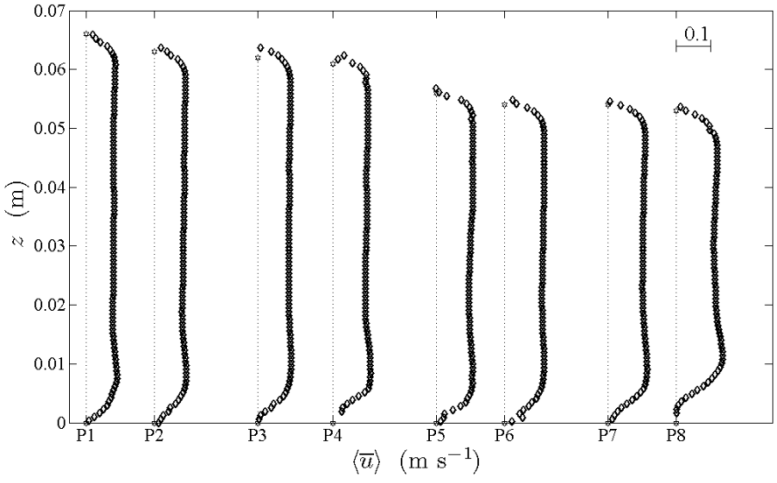

Figure 5 Vertical profiles of longitudinal velocity.

Figures 6, 7 and 8 compare Reynolds (black markers) and form induced stresses (red markers) for all longitudinal positions.One can, in general, conclude that turbulent and dispersive stresses have the same other of magnitude, proving that the later should not be neglected by comparison with the former. Figure 6 presents the longitudinal component of the normal form induced stresses, which is a good variable to identify the region, on the water column, where the flow is mainly controlled by the stems, once its profile shows inflection points where both the bottom and the free surface loose importance in the control of the flow. Longitudinal form-induced stresses translate the great heterogeneity of the flows within vegetation covered boundaries and its magnitude increases with the increasing of the stem density. Furthermore, Figure 6 shows profiles of longitudinal Reynolds stress which also increase with the stem

density. Comparing both stresses, it is observed that the form-induced stresses present, in general, higher values than the Reynolds stresses; however they have the same order of magnitude.

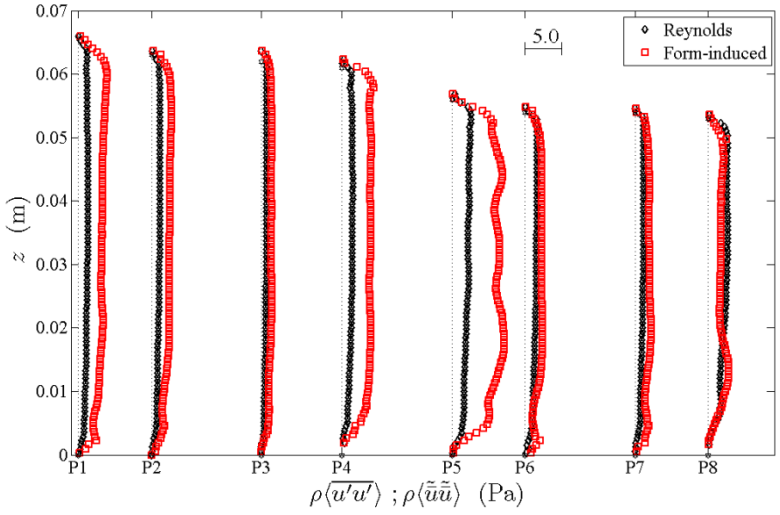

Figure 6 Vertical profiles of Reynolds and form-induced longitudinal normal stresses.

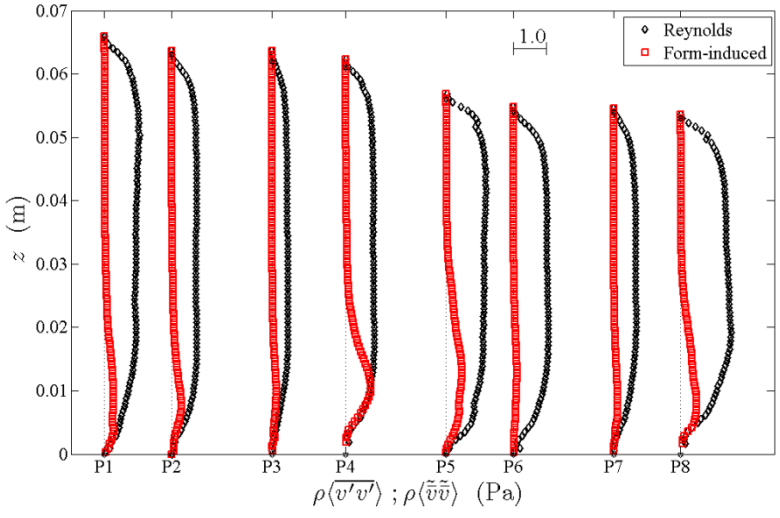

Figure 7 Vertical profiles of Reynolds and form-induced vertical normal stresses.

Figure 7presents profiles of vertical Reynolds and form induced stresses, showing that is also clear the correlation between those stresses and the density of stems. The Reynolds stresses have similar values for both of the normal stresses, however the vertical component of form induced stresses are approximately one order of magnitude smaller than the longitudinal one.

Concerning shear stresses, Figure 8 shows they are one order of magnitude smaller than normal stresses, both for turbulent and dispersive cases. Comparing the two kind of stresses one can observe they have the same order of magnitude with maximum values near the bottom and values very close to zero close to the free surface. Figure 8 also shows that shear stresses also increase with increasing stem density.

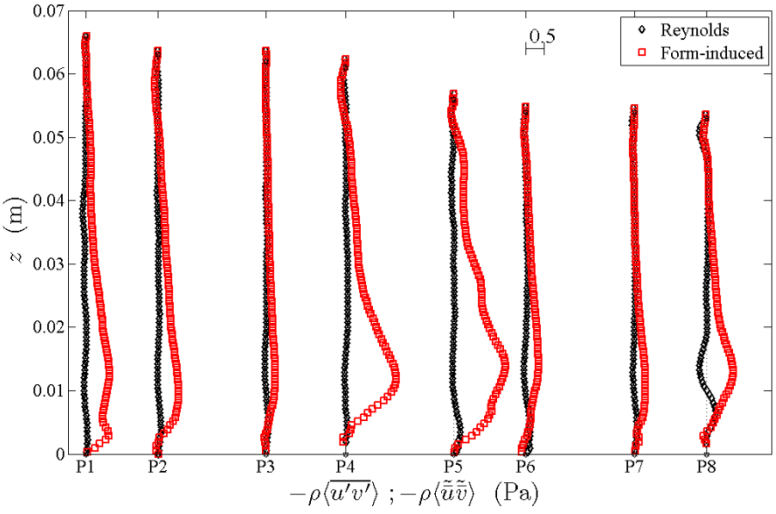

Figure 8 Vertical profiles of Reynolds and form-induced shear stresses.

Using equation (3) and applying the definition introduced above the drag coefficients was computed for each of the studied patches. The left-hand side ofFigure 9 represents the mean drag coefficient for each longitudinal positionshowing that a clear conclusion is difficult to draw, however it seems that there is a tendency for a decrease of the drag coefficient with the increase of the stem density. Tanino and Nepf (2009) reports a positive correlation between the drag coefficient and the stem density for Re_p<690 while Nepf (1999) shows an inverse relation between the two variables for Re_p>4000. The range of stem Reynolds number varies between 946 and 1298 in the present study and the drag coefficient varies in accordance to the work of Nepf (1999). Therefore it may be expectable that the stem density dependence of the drag coefficient reverses between Re_p=700 and Re_p=900. Concerning the relation between stem Reynolds number and drag coefficient (Figure 9-right), the later decreases when former increases, for patches with same stem density. It should be noticed that the drag coefficient for position P1 is not possible to compute once there were not measurements upstream of the position making unfeasible the computation of flow variable gradients.

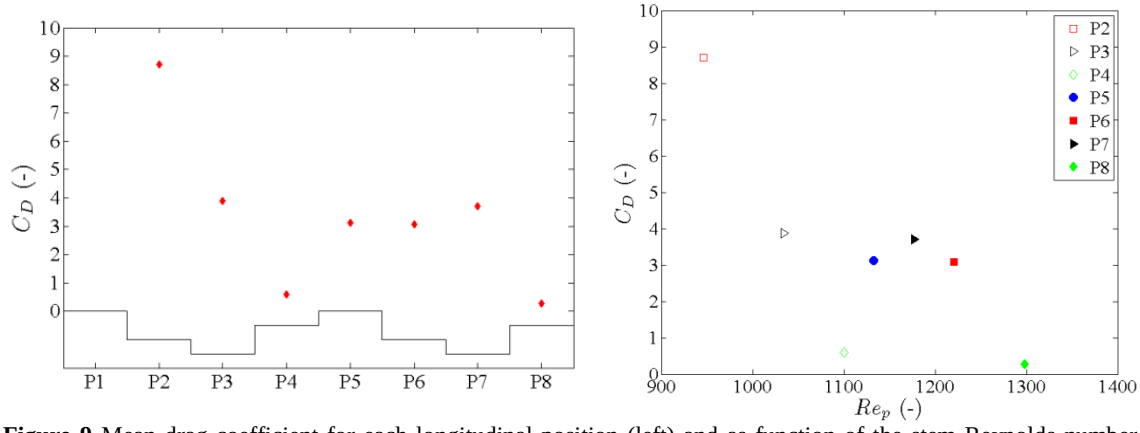

Figure 9 Mean drag coefficient for each longitudinal position (left) and as function of the stem Reynolds number (right). The solid line on the background of the figure on the left-hand side represents the stem density characteristic of each longitudinal position.

5 CONCLUSIONS

A characterization of the studied flow was carried out showing that flows within vegetation covered boundaries are characterized by great heterogeneity. One can conclude that the flow within a dense array

of stems leads a quasi-symmetric high vorticity patterns around the stemsindependently of the stem density. However, stem density impacts the length of the vortex street: for lower densities the inter-stem space is larger allowing the development of the vortex street.

Vertical profiles of velocity and stresses were computed according to the framework of the Double-Average methodology, leading to the following conclusions:

- There is a strong correlation between stem density and the magnitude of flow variables. Both turbulent and the form induced stresses increase with the density of the vertical elements.
- Form-induced stresses have the same order of magnitude of Reynolds stresses for both normal and shear components.
- Normal longitudinal stresses are dominant. The form-induced stresses are the main expression of flow heterogeneity and spatial anisotropy.
- The drag coefficient presents a tendency to decrease with the stem density.
- The drag coefficient decreases with the stems Reynolds number.

Additional experimental tests, with a wider range of Reynolds numbers, are required to validate the latter two conclusions.

ACKNOWLEDGEMENTS

This study was funded by the Portuguese Foundation for Science and Technology through the project PTDC/ECM/099752/2008 and PTDC/ECM/117660/2010.

REFERENCES

Ferreira, R. M. L., Ricardo, A. M. and Franca, M. J.,2009. Discussion of 'Laboratory investigation of mean drag in a random array of rigid, emergent cylinders' by Heydi M. Nepf and Yukie Tanino, Journal of Hydraulic Engineering, vol. 134, n. 1, 2008. Journal of Hydraulic Engineering 135(8).

Finnigan, J.,2000. Turbulence in plant canopies.Annu. Rev. Fluid Mech. 32, 519–571.

Giménez-Curto, L. and M. Corniero Lera, 1996. Oscillating turbulent flow over very rough surfaces. J. Geophys. Res. 101, 20745-20758.

Hjemfelt, A. T. and L. F. Mockros, 1996.Motion of discrete particles in a turbulent fluid.Applied Science Research 16, 149-161.

Nepf, H. M., 1999. Drag, turbulence, and diffusion in flow through emergent vegetation, Water Resources. Research, 35(2), 479–489.

Nikora, V., Goring, D., McEwan, I. and Griffiths, G, 2001.Spatially averaged open-channel flow over rough bed. Journal of Hydraulic Engineering 127(2), 123–133.

Nikora, V., McEwan, I., McLean, S., Coleman, S., Pokrajac, D. and Walters, R., 2007. Double-averaging concepts for rough-bed open-channel and overland flows: Theoretical background. Journal of Hydraulic Engineering 133(8), 873–883.

Raupach, M. R., P. A. Coppin, and B. J. Legg, 1986. Experiments on scalar dispersion within a model plant canopy part i: turbulence structure. Boundary Layer Meteorology 35, 21-52.

Tanino, Y. and H. M. Nepf, 2008. Lateral dispersion in a random cylinder array at high Reynolds number, J. Fluid Mech., 600, 339-371.